European Radiology (2019) 29:993–1002
https://doi.org/10.1007/s00330-018-5627-4

GASTROINTESTINAL

Diffusion and perfusion MRI quantification in ileal Crohn's disease

Stefanie J. Hectors[1,2] · Sonja Gordic[1,3] · Sahar Semaan[1,2] · Octavia Bane[1,2] · Robert Hirten[4] · Xiaoyu Jia[5] · Jean-Frederic Colombel[4] · Bachir Taouli[1,2]

Received: 13 March 2018 / Revised: 12 June 2018 / Accepted: 21 June 2018 / Published online: 17 July 2018

Abstract

Objectives To quantify intravoxel incoherent motion (IVIM)-DWI and dynamic contrast-enhanced (DCE)-MRI parameters in normal and abnormal ileal segments in Crohn's disease (CD) patients and to assess the association of these parameters with clinical and MRI-based measurements of CD activity.

Methods In this prospective study, 27 CD patients (M/F 18/9, mean age 42 years) underwent MR enterography, including IVIM-DWI and DCE-MRI. IVIM-DWI and DCE-MRI parameters were quantified in normal and abnormal small bowel segments, the latter identified by the presence of inflammatory changes. MRI parameter differences between normal and abnormal bowel were tested using Wilcoxon signed-rank tests. IVIM-DWI and DCE-MRI parameters were correlated with clinical data (C-reactive protein, Harvey-Bradshaw Index), conventional MRI parameters (wall thickness, length of involvement) and MRI activity scores (MaRIA, Clermont). Diagnostic performance of (combined) parameters for differentiation between normal and abnormal bowel was determined using ROC analysis.

Results The DCE-MRI parameters peak concentration C_{peak}, upslope, area-under-the-curve at 60s (AUC60), K^{trans} and v_e were significantly increased (p<0.023), while IVIM-DWI parameters perfusion fraction (PF) and ADC were significantly decreased (p<0.001) in abnormal bowel segments. None of the DCE-MRI and IVIM-DWI parameters correlated with clinical parameters (p>0.105). DCE-MRI parameters exhibited multiple significant correlations with wall thickness (C_{peak}, upslope, AUC60, K^{trans}; r range 0.431–0.664, p<0.025) and MaRIA/Clermont scores (C_{peak}, AUC60, K^{trans}; r range 0.441–0.617, p<0.021). Combined K^{trans}+v_e+PF+ADC showed highest AUC (0.963) for differentiation between normal and abnormal bowel, while ADC performed best for individual parameters (AUC=0.800).

Conclusions DCE-MRI and IVIM-DWI, particularly when used in combination, are promising for non-invasive evaluation of small bowel CD.

Key Points

- *IVIM-DWI and DCE-MRI parameters were significantly different between normal and abnormal bowel segments in CD patients.*
- *DCE-MRI parameters showed a significant association with wall thickness and MRI activity scores.*
- *Combination of IVIM-DWI and DCE-MRI parameters led to the highest diagnostic performance for differentiation between normal and abnormal bowel segments, while ADC showed the highest diagnostic performance of individual parameters.*

Keywords Crohn disease · Diffusion magnetic resonance imaging · Perfusion imaging

✉ Bachir Taouli
bachir.taouli@mountsinai.org

[1] Translational and Molecular Imaging Institute, Icahn School of Medicine at Mount Sinai, New York, NY, USA

[2] Department of Radiology, Icahn School of Medicine at Mount Sinai, New York, NY, USA

[3] Institute of Diagnostic and Interventional Radiology, University Hospital Zurich, Zurich, Switzerland

[4] IBD Center, Division of Gastroenterology, Department of Medicine, Icahn School of Medicine at Mount Sinai, New York, NY, USA

[5] Department of Population Health Science and Policy, Institute for Healthcare Delivery Science, Icahn School of Medicine at Mount Sinai, New York, NY, USA

Abbreviations

ADC	Apparent diffusion coefficient
AIF	Arterial input function
AUC60	Area under the curve at 60 s
[CA]	Contrast agent concentration
CD	Crohn's disease
CDEIS	Crohn's Disease Endoscopic Index of Severity
C_{peak}	Peak concentration
CRP	C-reactive protein
D	Diffusion coefficient
D*	Pseudodiffusion coefficient
DCE-MRI	Dynamic contrast-enhanced MRI
DWI	Diffusion-weighted imaging
HBI	Harvey-Bradshaw index
IVIM-DWI	Intravoxel incoherent motion diffusion-weighted imaging
k_{ep}	Wash-out constant
K^{trans}	Transfer constant
MaRIA	Magnetic Resonance Index of Activity
OR	Odds ratio
PF	Perfusion fraction
RCE	Relative contrast enhancement
ROI	Region of interest
SD	Standard deviation
SI	Signal intensity
T1WI	T1-weighted imaging
T2WI	T2-weighted imaging
TTP	Time-to-peak
VFA	Variable flip angle
v_p	Plasma volume fraction

Introduction

Crohn's disease (CD) is a chronic inflammatory bowel disease that can affect any part of the entire gastrointestinal tract, but most often involves the terminal ileum [1]. Colonoscopy is considered the reference standard for assessment of disease activity in patients with CD [2]. However, a limitation of endoscopy is that it only allows for evaluation of the mucosal surface without the possibility of evaluating transmural involvement and extraluminal complications, and that it has a limited role for assessment of the small bowel. Magnetic resonance (MR) enterography is becoming increasingly used as a non-invasive and radiation-free imaging technique for the diagnosis and monitoring of CD and for assessment of CD activity [3, 4]. MRI enables evaluation of the bowel outside the reach of the endoscope and may potentially provide a more accurate and reliable measurement of CD activity compared to endoscopy. Various MRI-based CD activity scores have been introduced, which are based on a combination of qualitative and quantitative MRI parameters. For example, the Magnetic Resonance Index of Activity (MaRIA) score, consisting of a composite measure of the presence of oedema and ulceration, wall thickness and contrast enhancement, has shown a strong correlation with Crohn's Disease Endoscopic Index of Severity (CDEIS) [5]. More recently, the Clermont score was introduced, which includes the apparent diffusion coefficient (ADC) measured with diffusion-weighted imaging (DWI) as a variable and eliminates the need for contrast-enhanced images for disease assessment. The Clermont score has shown strong correlation with the MaRIA score [6]. While the MRI-based CD activity scores are promising, quantitative functional MRI parameters may potentially allow for a more objective measurement of disease severity. Both pharmacokinetic (quantitative) and model-free (semi-quantitative) perfusion parameters from dynamic contrast-enhanced MRI (DCE-MRI) measurements have shown promise for evaluation of CD activity [7–11] and assessment of treatment response in CD [12, 13]. Intravoxel incoherent motion DWI (IVIM-DWI) is a DWI technique that allows for simultaneous assessment of tissue diffusion and pseudodiffusion due to capillary blood flow [14, 15]. IVIM-DWI may be an attractive alternative to contrast-enhanced acquisitions, as it allows for estimation of perfusion/flow and diffusion in a single acquisition without the need for injection of contrast. IVIM-DWI has been investigated in a previous study in paediatric CD patients, in which significant differences were found between IVIM-DWI parameters in normal, non-enhancing bowel and abnormal, enhancing bowel segments [16]. Thus, DCE-MRI and IVIM-DWI are both promising methods for evaluation of CD. However, no studies have combined IVIM-DWI and DCE-MRI into a single MRI protocol to compare the diagnostic performance of (combination of) these methods for the assessment of CD severity. In addition, IVIM-DWI and DCE-MRI have not been compared to the previously proposed MR-based CD activity scores.

The objectives of our study were to (1) quantify IVIM-DWI and DCE-MRI parameters in normal and abnormal ileal segments in CD patients and (2) to assess the association of IVIM-DWI and DCE-MRI parameters with clinical and MRI-based measurements of CD activity.

Materials and methods

Ethical considerations

This single-centre, prospective study was compliant with the Health Insurance Portability Act and approved by the local institutional review board. Written informed consent was obtained from all subjects.

Patients

Inclusion criteria were CD patients with (1) a suspicion of active disease in the small bowel based on physician notes,

endoscopy and laboratory data, including C-reactive protein (CRP) and (2) a clinical MR enterography scheduled. The subjects consented to have research MRI sequences (IVIM-DWI and DCE-MRI) added to their clinical MRI scan. Clinical disease activity was determined by the Harvey-Bradshaw index (HBI) [17]. HBI scores were determined by a gastroenterologist specializing in inflammatory bowel disease (RH) by evaluation of clinical data from office visits within 3 months of the MRI examination. CRP values obtained within a 3-month interval of the MRI examination were recorded from the medical charts, where available.

MRI acquisition

The MRI acquisition was performed at either 1.5T (Aera, Siemens Healthineers; n=21) or 3.0T (Skyra, Siemens Healthineers; n=6). Patients were requested to fast for 6 h before the MRI. To achieve adequate small bowel distension, three bottles of Volumen (E-Z-EM) were given orally, beginning 45 min before the MRI examination. To reduce bowel peristalsis, 1 mg of glucagon was administered intramuscularly before the MRI acquisition (except in diabetic patients). Clinical MRI assessment of the bowel consisted of axial and coronal T_2-weighted HASTE imaging (T2WI) without fat-suppression, axial T_1-weighted in-phase and out-of-phase imaging, axial 3D T_1-weighted VIBE gradient echo imaging (T1WI) before contrast and axial and coronal T_1-weighted VIBE at 3–4 min after contrast injection. The acquisition parameters of the IVIM-DWI and DCE-MRI scans are shown in Table 1. A variable flip angle (VFA) T_1 mapping acquisition was performed to provide baseline T_1 measurements for the DCE-MRI modelling (Table 1). Gadoterate meglumine (Dotarem, Guerbet) 0.1 mmol/kg was injected at 25 s after the start of the DCE-MRI acquisition at a rate of 2 ml/s, followed by a 20-ml saline flush at the same rate. The DCE-MRI acquisition was performed until 3 min after injection.

Clinical MRI analysis

A body radiologist (observer 1, SS, with 2 years of experience in body MRI) reviewed the MRI images, blinded to clinical data and the IVIM-DWI and DCE-MRI images and results. For the largest involved ileal segment in each patient, the length of the involved small bowel segment and the wall thickness (from T1WI) were determined. Bowel wall was considered abnormal if the wall thickness was > 3 mm in a well-distended bowel wall segment [18]. In addition, the presence of ulceration(s) and oedema were noted. Ulcerations were defined as deep depressions in the mucosal surface of the thickened segment [5]. Oedema was diagnosed by the presence of hyperintensity of the small bowel wall relative to the signal of psoas muscle on T2WI [5]. Presence of additional signs such as small bowel strictures, penetrating disease and abscesses were noted.

In addition, the MaRIA and Clermont scores [5, 6, 19] were calculated as :

$$\mathrm{MaRIA} = 1.5 \times \text{wall thickness} + 0.02 \times \mathrm{RCE} + 5 \times \text{oedema} + 10 \times \text{ulceration}$$

$$\mathrm{Clermont} = 1.646 \times \text{wall thickness} - 1.321 \times \mathrm{ADC} + 5.613 \times \text{oedema} + 8.306 \times \text{ulceration} + 5.039$$

Small bowel wall thickness (in mm) was measured on contrast-enhanced T_1 VIBE images. Small bowel wall ADC was measured as described below. RCE represents the relative contrast enhancement and was derived from dynamic signal intensity (SI) curves from the DCE-MRI acquisition. The mean SI in the region of interest (ROI) of abnormal bowel

Table 1 Acquisition parameters of the intravoxel incoherent motion diffusion-weighted imaging (IVIM-DWI), T1 variable flip angle (VFA) and dynamic contrast-enhanced (DCE)-MRI acquisitions. Parameters were kept the same between 1.5T and 3.0T unless specified otherwise

Parameter	IVIM-DWI	T1 VFA	DCE-MRI
Sequence type	Single-shot SE-EPI	3D FLASH	3D FLASH
Echo time (ms)	83 (1.5T)/81 (3.0T)	1.21 (1.5T)/1.13 (3.0T)	1.03 (1.5T)/0.89 (3.0T)
Repetition time (ms)	6000	3.52 (1.5T)/3.50 (3.0T)	2.67 (1.5T)/2.7 (3.0T)
Flip angle (°)	90	2, 10	11.5
Matrix	192*138	384*252	192*144
Field of view (mm^2)	380*273	360*236	360*270
Number of slices	56	40	72
Slice thickness (mm)	6	3	3
Number of averages	1, 2, 2, 2, 2, 2, 2, 2	1	1
b-values (s/mm^2)	0, 25, 50, 75, 100, 200, 400, 800	-	-
Acquisition time (min:s)	9:00	0:14	0:03/dynamic

FLASH fast low angle shot, *SE-EPI* spin-echo echo planar imaging

wall tissue drawn for the DCE-MRI analysis (see below) was taken. RCE was calculated as 100*(SI 70 s post-contrast – SI pre-contrast)/SI pre-contrast, with the assumption that the noise was constant throughout the DCE-MRI acquisition. The DCE-MRI images obtained at 70 s were used for RCE calculation as suggested previously [5].

DCE-MRI and IVIM-DWI analysis

ROIs were drawn in 1–2 slices in the abnormal, involved bowel segment and in a remote normal-looking bowel segment on the IVIM-DWI images using OsiriX software (Pixmeo) and on the DCE-MRI images using FireVoxel software (CAI^{2}R, New York University). The ROI in the abnormal bowel segment, defined during the clinical MRI analysis, was drawn in the region of greatest wall thickness. The ROI placement was performed by observer 2 (SG, a radiologist with 1 year of experience in body MRI) or observer 3 (SJH, an MR physicist with 2 years of experience in body MRI). A representative example of the ROI placement is shown in Fig. 1.

For DCE-MRI analysis, additional ROIs were placed in the abdominal aorta below the renal bifurcation to determine the arterial input function (AIF) and in the psoas muscle as reference tissue for AIF correction, as described earlier [20, 21]. SI curves in the normal bowel, abnormal bowel and aorta were converted to dynamic contrast agent concentration ([CA]) curves by using the signal equation for a spoiled gradient echo sequence, pre-contrast T_1 values from the T_1 VFA scan and the contrast agent's relaxivity [22]. For the aorta, pre-contrast T_1 values were based on the literature [23]. A haematocrit value of 0.45 was used for conversion from blood [CA] to plasma [CA]. Quantitative DCE-MRI analysis was performed using custom-written scripts in MATLAB (version R2016b, MathWorks). The extended Tofts model was fitted to the dynamic [CA] curves in the normal and abnormal bowel ROIs to estimate transfer constant K^{trans}, wash-out constant k_{ep} and plasma volume fraction v_p [24]. The extravascular extracellular volume fraction v_e was derived from the model parameters by dividing K^{trans} by k_{ep}. In addition to the quantitative pharmacokinetic DCE-MRI parameters, semi-quantitative model-free parameters were obtained: time-to-peak (TTP, s), peak concentration (C_{peak}, mM), area under the curve at 60 s (AUC60, mM*s) and upslope (mM/s).

For modelling of the IVIM-DWI data, the biexponential IVIM model [14, 25] was fitted to the mean signal curves in the ROIs at the different b-values to estimate pseudodiffusion coefficient D*, diffusion coefficient D and perfusion fraction PF using a Bayesian fitting algorithm [26] written in MATLAB. The apparent diffusion coefficient (ADC) was determined by calculation of the slope of a linear fit through the logarithmic signal data at b=50, 400 and 800 s/mm^2, reflecting b-values that are typically used for DWI in clinical MR enterography protocols [19]. An example of the DCE-MRI and IVIM-DWI fitting is shown in Fig. 1.

Statistical analysis

The Kolmogorov-Smirnov test indicated that not all MRI parameters showed normality (p-values 0.022 for v_p, 0.003 for

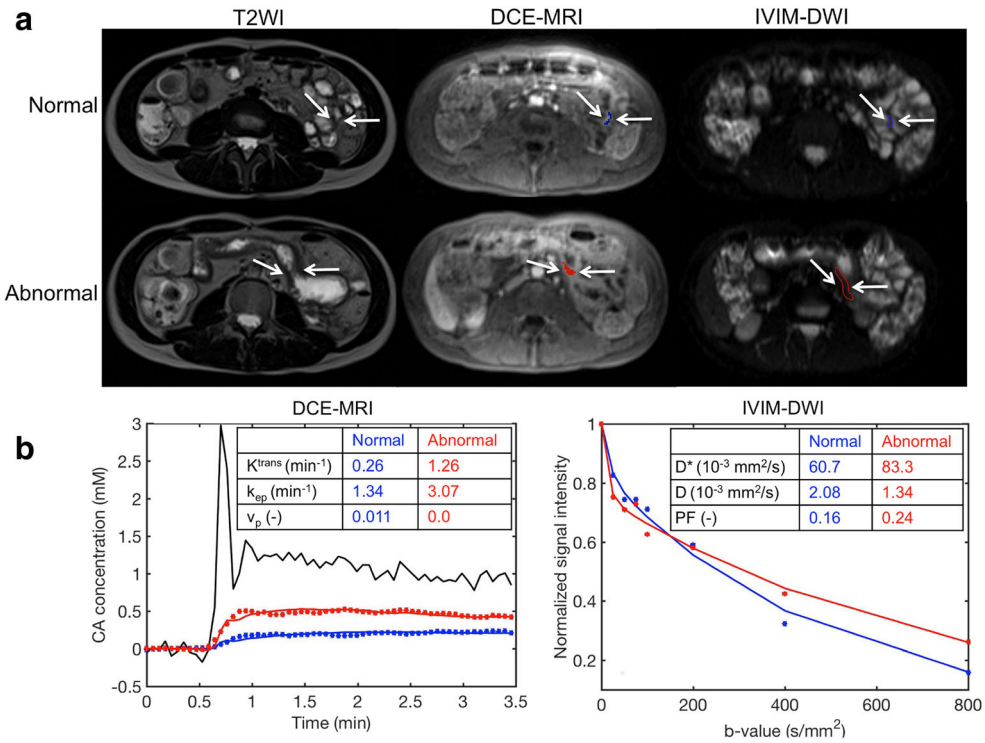

Fig. 1 Dynamic contrast-enhanced (DCE)-MRI and intravoxel incoherent motion (IVIM)-DWI processing of abnormal and normal bowel segments in a 22-year-old female Crohn's disease patient. (**a**) Location of normal and abnormal bowel segments on T2WI, DCE-MRI and IVIM-DWI (b=0 s/mm^2) images (white arrows). The abnormal bowel segment was characterised by wall thickening. Region of interest (ROI) placement in normal (blue) and abnormal (red) bowel wall segments is shown on the DCE-MRI and IVIM-DWI images. (**b**) DCE-MRI and IVIM-DWI fits (solid lines) and data points in the normal (blue) and abnormal bowel (red) ROIs with corresponding estimated parameters. The arterial input function is shown in black on the DCE-MRI plot

D*, 0.007 for upslope in the normal bowel and 0.001 for v_e, 0.021 for upslope in the abnormal bowel). Therefore, non-parametric tests were used for the statistical analysis.

Differences in DCE-MRI and IVIM-DWI parameters between normal and abnormal bowel segments were tested for statistical significance using Wilcoxon signed-rank tests. ROC analysis was performed to determine the diagnostic performance of each of the parameters for differentiation between normal and inflamed bowel segments (based on qualitative evaluation). General linear modelling with stepwise feature selection (inclusion *p*-value 0.05, exclusion *p*-value 0.1) was employed to find the best combination of IVIM-DWI and/or DCE-MRI parameters for assessment of abnormal bowel. AUCs were compared using a DeLong test.

To assess synergy/redundancy between the IVIM-DWI and DCE-MRI parameters, Spearman correlations between the parameters were calculated.

Spearman analysis was also employed to assess the correlation of IVIM-DWI/DCE-MRI parameters in abnormal bowel segments with clinical parameters (CRP, HBI), conventional MRI measurements (length of involvement, wall thickness) and MRI activity scores (MaRIA and Clermont). In order to determine whether quantitative MRI could provide alternatives to more subjective MRI scores, general linear modelling with stepwise feature selection was employed to determine the optimal combination of parameters to predict MaRIA and Clermont scores. The predicted values from the built general linear models were correlated with measured MaRIA and Clermont scores using Pearson correlation analysis. Agreement between measured and predicted MaRIA and Clermont scores was assessed by the Lin's concordance correlation coefficient.

Univariate (and multivariate, where applicable) logistic regression analysis was performed to assess the association of the MRI parameters in abnormal bowel segments with presence of oedema, ulceration or severe disease (MaRIA > 11). Prior to logistic regression analysis, IVIM and DCE-MRI parameters were standardised (mean 0, standard deviation (SD) 1) to facilitate comparison between odds ratios (ORs) of different parameters. For all tests, a *p*-value <0.05 was considered significant.

Results

Patients

From December 2015 to October 2017, 48 patients were included in our study, of which 17 patients did not show an MRI-visible region of active disease in the small bowel and four patients did not have DCE-MRI. The 27 included patients (M/F 18/9) had an average age of 42 years (range 21–69 years). Ten of the patients (37%) had prior small bowel surgery. Fourteen patients (52%) were receiving anti-TNF therapy at the time of the MRI scan.

Clinical and MRI characteristics

Clinical and MRI characteristics of the included patients are shown in Table 2. CRP values within a 3-month time window from the MRI were available for 23 patients (average time between CRP measurements and MRI 30 days, range 2–70 days). HBI scores could be calculated for 19 patients (average time between HBI and MRI 34 days, range 6–95 days). Most patients (n=23, 85%) were classified as having severe disease according to the MaRIA score (MaRIA>11), mostly associated with the presence of ulceration and/or oedema.

For the DCE-MRI parameters, significantly increased C_{peak} ($p<0.001$), upslope ($p=0.023$), AUC60 ($p<0.001$), K^{trans} ($p=0.009$) and v_e ($p=0.009$) were observed in abnormal versus normal bowel segments (Fig. 2). IVIM-DWI parameters showed a significantly decreased PF ($p=0.001$) and ADC ($p<0.001$) in the abnormal bowel segments (Fig. 2). Results of ROC analysis for differentiation between normal and abnormal bowel are shown in Table 3. For individual parameters, ADC showed the best diagnostic performance for prediction of diseased bowel (AUC=0.800). General linear modelling with stepwise feature selection selected only AUC60 as a

Table 2 Clinical and MRI characteristics of patient population (n=27)

Characteristic	Value
Serum CRP* (mg/L)	18.0 ± 25.8 (range 0.3–115.6)
Length of involvement (cm)	11.1 ± 5.5 (range 4.4–24.9)
HBI#	3.3 ± 3.6 (range 0–12)
Wall thickness (mm)	8.1 ± 2.6 (range 3.1–12.9)
ADC (10^{-3} mm^2/s)	1.47 ± 0.36 (range 0.86–2.30)
RCE (%)	125.8 ± 62 (range 8.1–268)
Oedema	
- Absent	5 (19%)
- Present	22 (81%)
Ulceration	
- Absent	6 (22%)
- Present	21 (78%)
MaRIA	26.5 ± 9.1 (range 6.8–37.2)
Clermont	27.4 ± 8.2 (range 8.8–38.2)
Severe disease (MaRIA > 11)	
- No	4 (15%)
- Yes	23 (85%)

Data are presented as means ± standard deviation

ADC apparent diffusion coefficient, *CRP* C-reactive protein, *HBI* Harvey-Bradshaw Index, *MaRIA* Magnetic Resonance Index of Activity, *RCE* relative contrast enhancement

*CRP values were available for 23 patients

HBI scores were calculated for 19 patients

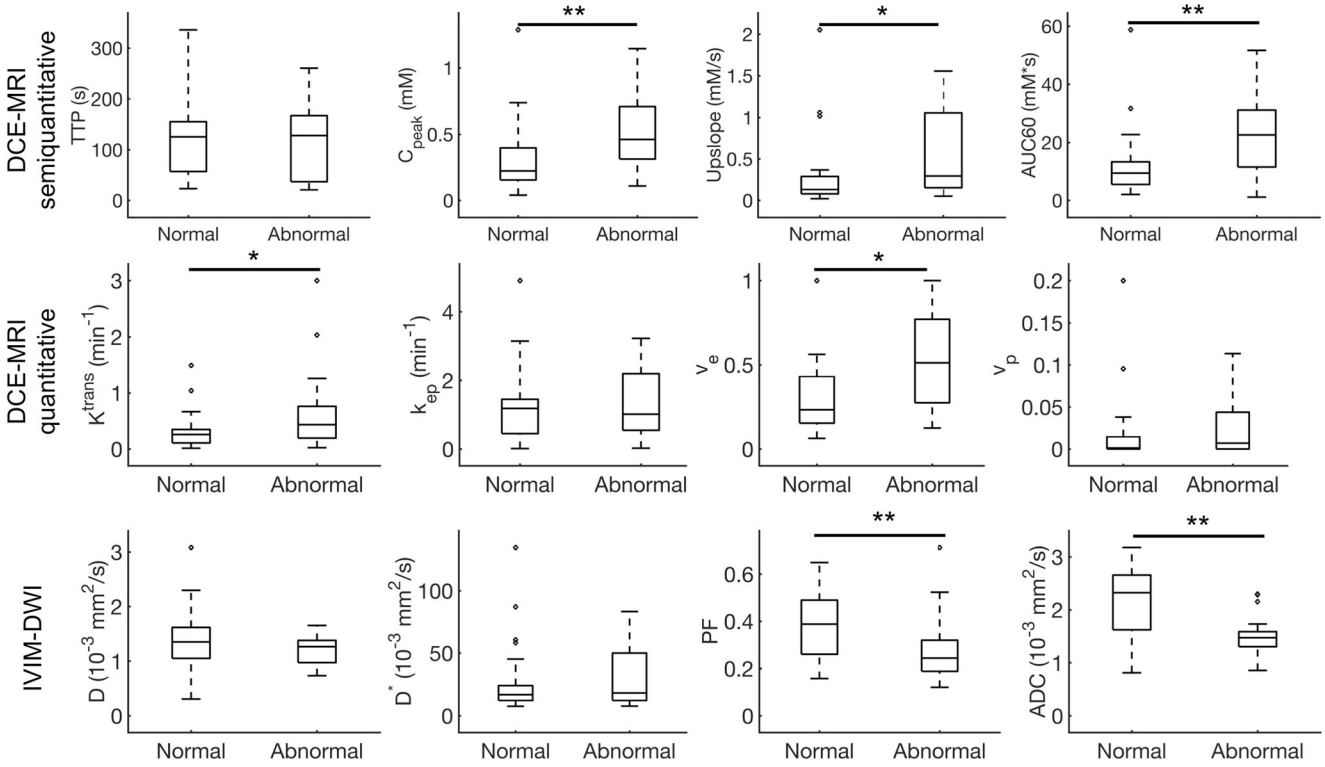

Fig. 2 Box plots of the dynamic contrast-enhanced (DCE)-MRI and intravoxel incoherent motion (IVIM)-DWI parameters in normal and abnormal bowel segments of the 27 included patients with Crohn's disease. * and ** indicate a significant difference between normal and abnormal bowel with $p<0.05$ and $p<0.001$, respectively (Wilcoxon signed-rank test)

Table 3 Receiver operating characteristic analysis results for differentiation of normal and abnormal bowel segments

Parameter	AUC	*p*	Cut-off	Sensitivity	Specificity
DCE-MRI					
TTP (s)	0.534	0.672	136.9	70.4%	44.4%
C_{peak} (mM)	0.733	**0.003**	0.41	66.7%	81.5%
Upslope (mM/s)	0.693	**0.015**	0.17	74.1%	73.0%
AUC60 (mM*s)	0.733	**0.003**	21.0	44.4%	88.9%
K^{trans} (min^{-1})	0.694	**0.014**	0.35	66.7%	77.8%
k_{ep} (min^{-1})	0.527	0.736	1.54	37.0%	77.8%
v_e	0.704	**0.010**	0.45	55.6%	81.5%
v_p	0.583	0.295	0.001	70.4%	51.9%
IVIM-DWI					
D (10^{-3} mm^2/s)	0.609	0.169	1.39	77.8%	48.1%
D* (10^{-3} mm^2/s)	0.549	0.539	21.9	44.4%	74.1%
PF	0.734	**0.003**	0.356	85.2%	63.0%
ADC (10^{-3} mm^2/s)	0.800	**<0.001**	1.77	88.9%	70.4%
PF + ADC	0.885	**<0.001**	0.75	66.7%	96.3%
Combined parameters					
K^{trans} + v_e + PF + ADC	0.963	**<0.001**	0.69	88.9%	100%

Significant *p*-values are bolded

ADC apparent diffusion coefficient, *AUC60* area under the curve at 60 s, C_{peak} peak concentration, *D* diffusion coefficient, *D** pseudodiffusion coefficient, k_{ep} wash-out constant, K^{trans} transfer constant, *PF* perfusion fraction, *TTP* time-to-peak, v_e extravascular extracellular volume fraction, v_p plasma volume fraction

significant predictor for bowel inflammation when only DCE-MRI parameters were included, with an AUC of 0.733, while the combination of IVIM-DWI parameters PF + ADC showed an AUC of 0.885. The highest AUC was observed when combining DCE-MRI and IVIM parameters K^{trans}, v_e, PF and ADC with an observed AUC of 0.963. This combination of parameters had a significantly higher AUC than ADC alone (DeLong test p=0.012) and PF + ADC (p=0.043). In terms of correlations between IVIM-DWI and DCE-MRI parameters, significant negative correlations were observed between Upslope and PF (r=-0.294, p=0.031) and between v_p and ADC (r=-0.286, p=0.036).

Association of IVIM-DWI and DCE-MRI parameters with clinical and MRI characteristics

Table 4 shows the correlations of DCE-MRI/IVIM-DWI parameters with clinical and conventional MRI characteristics and MRI activity scores of the included patients. IVIM-DWI parameters did not show any significant correlation with any of the assessed parameters. None of the parameters showed significant correlation with CRP values, HBI and length of involvement. DCE-MRI parameters C_{peak}, upslope, AUC60 and K^{trans} showed significant moderate-to-strong correlations with wall thickness. The semi-quantitative DCE-MRI parameters C_{peak} and AUC60 showed significant moderate-to-strong correlations with the MaRIA and Clermont scores, while K^{trans} only significantly correlated with Clermont score.

The combination of C_{peak} and D were shown to be the most significant predictors for MaRIA and Clermont scores using general linear modelling (Fig. 3). The estimates from the general linear model using this combination of parameters showed strong correlations (r=0.741 and 0.738, respectively, p<0.001) and good agreement (Lin's correlation coefficient 0.709 and r=0.705, respectively) with the measured MaRIA and Clermont scores. Logistic regression analysis showed strong associations of C_{peak} and AUC60 with presence of oedema, between D and presence of ulceration, and between C_{peak} and the presence of severe disease (MaRIA > 11; Table 5). Multivariate analysis did not show an added value of the combination of C_{peak} and AUC60 for prediction of presence of oedema compared to C_{peak} alone (p=0.266).

Discussion

Our study assessed the utility of DCE-MRI and IVIM-DWI parameters for non-invasive assessment of CD activity. While both methods have shown promising results for assessment of severity of CD [7–11, 16], our study is the first to assess the value of combined DCE-MRI and IVIM-DWI measurements for the evaluation of CD. We found that both DCE-MRI and IVIM-DWI parameters showed significant differences between normal and abnormal bowel segments and that several DCE-MRI parameters showed significant associations with previously described MRI-based measurements of disease

Table 4 Correlations of dynamic contrast-enhanced (DCE)-MRI and intravoxel incoherent motion diffusion-weighted imaging (IVIM-DWI) parameters with clinical characteristics, conventional MRI parameters and MRI activity scores

Parameter	CRP	HBI	Length of involvement	Wall thickness	MaRIA	Clermont
DCE-MRI						
TTP (s)	r=-0.347, p=0.105	r=0.059, p=0.810	r=-0.025, p=0.903	r=-0.059, p=0.769	r=0.036, p=0.859	r=0.016, p=0.936
C_{peak} (mM)	r=-0.288, p=0.182	r=0.116, p=0.637	r=0.129, p=0.523	r=0.664, **p<0.001**	r=0.569, **p=0.002**	r=0.617, **p<0.001**
Upslope (mM/s)	r=0.114, p=0.606	r=0.088, p=0.721	r=0.076, p=0.706	r=0.431, **p=0.025**	r=0.306, p=0.120	r=0.356, p=0.069
AUC60 (mM*s)	r=-0.222, p=0.308	r=0.035, p=0.887	r=0.101, p=0.616	r=0.582, **p=0.001**	r=0.504, **p=0.008**	r=0.559, **p=0.003**
K^{trans} (min^{-1})	r=-0.214, p=0.327	r=0.131, p=0.592	r=0.338, p=0.085	r=0.447, **p=0.020**	r=0.372, p=0.056	r=0.441, **p=0.021**
k_{ep} (min^{-1})	r=0.027, p=0.904	r=0.069, p=0.779	r=0.267, p=0.178	r=0.254, p=0.201	r=0.263, p=0.184	r=0.269, p=0.175
v_e	r=-0.285, p=0.187	r=-0.143, p=0.560	r=0.123, p=0.541	r=0.283, p=0.152	r=0.069, p=0.733	r=0.185, p=0.357
v_p	r=0.213, p=0.329	r=0.090, p=0.714	r=-0.339, p=0.083	r=-0.059, p=0.772	r=-0.099, p=0.623	r=-0.139, p=0.488
IVIM-DWI						
D (10^{-3} mm^2/s)	r=0.085, p=0.700	r=-0.048, p=0.847	r=0.305, p=0.121	r=0.232, p=0.245	r=0.309, p=0.117	r=0.255, p=0.198
D* (10^{-3} mm^2/s)	r=0.021, p=0.923	r=-0.247, p=0.307	r=0.040, p=0.843	r=0.209, p=0.296	r=0.185, p=0.354	r=0.227, p=0.255
PF	r=-0.207, p=0.344	r=0.206, p=0.397	r=-0.151, p=0.454	r=-0.251, p=0.206	r=-0.209, p=0.293	r=-0.177, p=0.375
ADC (10^{-3} mm^2/s)	r=0.048, p=0.828	r=0.111, p=0.651	r=0.304, p=0.123	r=0.051, p=0.799	r=0.170, p=0.394	r=0.084, p=0.675

Significant p-values are given in bold type

ADC apparent diffusion coefficient, *AUC* area under the curve, *AUC60* area-under-the-curve at 60 s, C_{peak} peak concentration, *CRP* C-reactive protein, *D* diffusion coefficient, *D** pseudodiffusion coefficient, *HBI* Harvey-Bradshaw Index, k_{ep} wash-out constant, K^{trans} transfer constant, *MaRIA* Magnetic Resonance Index of Activity, *PF* perfusion fraction, *TTP* time-to-peak, v_e extravascular extracellular volume fraction, v_p plasma volume fraction

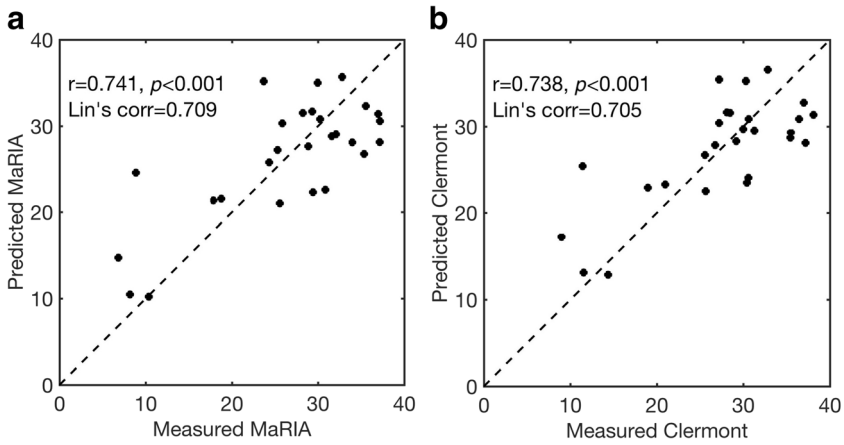

Fig. 3 Correlation plots between measured and predicted Magnetic Resonance Index of Activity (MaRIA) (**a**) and Clermont (**b**) scores. The predicted scores resulted from general linear modelling with stepwise feature selection. Predicted MaRIA score = -20.4 + 31989 * D + 61.35 * C_{peak} - 38065 * C_{peak} * D. Predicted Clermont score = -14.2 + 28080 * D + 56.70 * C_{peak} - 35146 * C_{peak} * D

activity. Combined DCE-MRI and IVIM-DWI parameters seem promising as an alternative for the more subjective MaRIA and Clermont MRI activity scores.

The significant increase in perfusion parameters C_{peak}, upslope, AUC60, K^{trans} and v_e in the abnormal bowel segments is supported by previous studies [7, 8] and is most likely related to angiogenesis in the inflamed bowel wall [8, 27]. The semi-quantitative DCE-MRI parameters C_{peak} and AUC60 showed strong correlations with conventional MRI measurements and scores of CD activity (wall thickness, MaRIA and Clermont scores) and were significantly associated with the presence of oedema. These results indicate the potential clinical utility of semi-quantitative DCE-MRI parameters for the non-invasive assessment of CD severity. An earlier study also found that semi-quantitative DCE-MRI parameters were more associated with disease activity in perianal fistulising CD than quantitative pharmacokinetic DCE-MRI parameters [11].

While there are a few studies that have assessed the use of DCE-MRI in CD [7–13], reports on IVIM-DWI in CD patients are limited. One previous study has explored the use of IVIM-DWI in paediatric CD [16]. The authors found a significantly higher D* and lower PF in enhancing versus non-enhancing bowel segments [16]. In our study, we also found a significantly lower PF in abnormal versus normal bowel segments and a non-significant increase in D*. The lower PF in affected bowel seems counterintuitive, given the higher perfusion in inflamed bowel. However, this is supported by an earlier finding of a reduction of microvascular volume in affected bowel segments in patients with inflammatory bowel disease, including CD, that was measured by examination of postoperative barium sulphate-perfused bowel segments [28]. The higher perfusion in inflamed bowel found in DCE-MRI parameters is thus likely not related to an increase in vascularity, but rather to an increase in blood flow to supply the diseased, inflamed tissue. The observed strong reduction of ADC in abnormal bowel segments has been reported in previous studies [10, 16, 29–31]. Diffusion restriction in inflamed bowel is likely related to infiltration of inflammatory cells, dilated lymphatic channels and granuloma development [29]. While the (IVIM-)DWI parameters showed promise for differentiation between normal and abnormal bowel, these parameters did not exhibit significant correlation with clinical and MRI-based parameters of CD severity (except for a moderate positive association between D and the presence of ulceration).

The IVIM-DWI and DCE-MRI parameters were in good agreement with values reported in previous studies on advanced MRI in CD with similar cohort sizes [8, 10, 11, 13, 16]. While these previous studies assessed DCE-MRI or IVIM-DWI in isolation for CD characterization, our study focused on the potential improved diagnostic performance of these techniques when used in combination. Only a few significant moderate correlations were found between the DCE-MRI and IVIM-DWI parameters in the bowel segments, showing that these techniques provide non-redundant information on tissue properties. Combination of K^{trans}, v_e, PF and ADC exhibited a significantly higher AUC for differentiation between normal and abnormal bowel compared to ADC alone. This finding suggests that a combination of quantitative DCE-MRI parameters, IVIM-DWI and conventional ADC measurements enhances contrast between normal and

Table 5 Univariate logistic regression analysis for prediction of oedema, ulceration or severe disease [Magnetic Resonance Index of Activity (MaRIA) >11]

Parameter	OR (95% CI)	*p*
Oedema		
C_{peak}	66.2 (1.8–2461)	0.023
AUC_{60}	10.9 (1.07–111.6)	0.044
Ulceration		
D	4.01 (1.18–13.7)	0.026
Severe disease		
C_{peak}	83.1 (1.17–5916.1)	0.042

AUC60 area under the curve at 60 s, C_{peak} peak concentration, *D* diffusion coefficient, *OR* odds ratio

inflamed bowel, which indicates the potential value of combined DCE-MRI and IVIM-DWI measurements for clinical assessment of CD. In addition, a general linear model combining C_{peak} and D showed strong correlation and good agreement with MaRIA and Clermont scores, which suggests that such a combination of quantitative MRI parameters could be used as a more objective alternative to these previously reported MRI scores for CD activity.

While conventional clinical assessment of MR enterography as well as the recently introduced MRI activity scores have shown promising results for assessment of CD severity [3], a main advantage of the use of MRI perfusion and diffusion methods is the ability of these techniques to provide objective, quantitative and spatially encoded information of entire bowel segments. In addition to the assessment of disease severity, the DCE-MRI and IVIM-DWI metrics may have utility for the assessment of CD response to therapy. In addition to DCE-MRI and IVIM-DWI, other quantitative MRI techniques such as magnetization transfer imaging have been recently described in CD [32].

The long acquisition time of 9 min for IVIM-DWI may be unfeasible for clinical MR enterography exams. It was beyond the scope of our study to assess whether a shorter acquisition with less b-values could be used without affecting the accuracy of IVIM parameter estimation. Post-processing of the IVIM-DWI and DCE-MRI images may be accelerated by using the same software for ROI placement and parameter quantification. In our study, we used different software packages for the different steps of post-processing. We expect that the entire post-processing could be completed within approximately 10 min when using an optimized graphical user interface.

None of the IVIM-DWI and DCE-MRI parameters were significantly correlated with clinical data (CRP and HBI). A previous study has shown significant associations of K^{trans}, v_e and ADC with CRP [10]. An explanation for the lack of correlation with clinical characteristics in our study may be the relatively long delay between the clinical measurements and the MRI examination (on average approximately 30 days). Particularly for the patients that were on concurrent anti-TNF treatment, the clinical parameters may have changed during that time course.

Our study had several limitations. First, the sample size was small, limiting validation of the general linear models of combined parameters in a separate validation cohort. Second, we did not correlate our findings with histopathology, which will be part of a separate study in which patients scheduled for bowel resection will be included. Third, there was a selection bias in the analysis of diagnostic performance of the MRI parameters for differentiation between normal and abnormal bowel, because intentionally the largest affected bowel segment was chosen in each patient. This could have led to overestimation of the diagnostic performance of the MRI parameters for differentiation between normal and abnormal bowel. In addition, clinical parameters (CRB and HBI) were not available for all patients.

In conclusion, DCE-MRI and IVIM-DWI parameters, particularly when used in combination, are promising for non-invasive evaluation of small bowel CD. The exact role of DCE-MRI and IVIM-DWI for CD management should be assessed in a larger cohort with histopathological validation.

Funding This study has received funding by research grants from Guerbet LLC and the Sanford J Grossman Charitable Trust for Integrative Studies in IBD at Mount Sinai.

Compliance with ethical standards

Guarantor The scientific guarantor of this publication is Bachir Taouli, MD.

Conflict of interest The authors of this manuscript declare relationships with the following companies: Jean-Frederic Colombel is a consultant for AbbVie, Amgen, Boehringer-Ingelheim, Celgene Corporation, Celltrion, Enterome, Ferring, Genentech, Janssen and Janssen, Medimmune, Merck & Co., Pfizer, Protagonist, Second Genome, Seres, Shire, Takeda and Theradiag, a speaker for AbbVie, Ferring and Speaker's bureau for Amgen and received grant support from AbbVie, Takeda and Janssen and Janssen. Bachir Taouli received grant support from Guerbet and Bayer.

Statistics and biometry One of the authors has significant statistical expertise.

Informed consent Written informed consent was obtained from all subjects (patients) in this study.

Ethical approval Institutional Review Board approval was obtained.

Methodology
- prospective
- observational
- performed at one institution

References

1. Peyrin-Biroulet L, Loftus EV Jr, Colombel JF, Sandborn WJ (2010) The natural history of adult Crohn's disease in population-based cohorts. Am J Gastroenterol 105:289–297
2. Van Assche G, Dignass A, Reinisch W et al (2010) The second European evidence-based Consensus on the diagnosis and management of Crohn's disease: Special situations. J Crohns Colitis 4:63–101
3. Bhatnagar G, Von Stempel C, Halligan S, Taylor SA (2017) Utility of MR enterography and ultrasound for the investigation of small bowel Crohn's disease. J Magn Reson Imaging 45:1573–1588
4. Coimbra AJ, Rimola J, O'Byrne S et al (2016) Magnetic resonance enterography is feasible and reliable in multicenter clinical trials in patients with Crohn's disease, and may help select subjects with active inflammation. Aliment Pharmacol Ther 43:61–72
5. Rimola J, Ordas I, Rodriguez S et al (2011) Magnetic resonance imaging for evaluation of Crohn's disease: validation of parameters of severity and quantitative index of activity. Inflamm Bowel Dis 17:1759–1768

6. Hordonneau C, Buisson A, Scanzi J et al (2014) Diffusion-weighted magnetic resonance imaging in ileocolonic Crohn's disease: validation of quantitative index of activity. Am J Gastroenterol 109:89–98
7. Florie J, Wasser MN, Arts-Cieslik K, Akkerman EM, Siersema PD, Stoker J (2006) Dynamic contrast-enhanced MRI of the bowel wall for assessment of disease activity in Crohn's disease. AJR. Am J Roentgenol 186:1384–1392
8. Oto A, Kayhan A, Williams JT et al (2011) Active Crohn's disease in the small bowel: evaluation by diffusion weighted imaging and quantitative dynamic contrast enhanced MR imaging. J Magn Reson Imaging 33:615–624
9. Tielbeek JA, Ziech ML, Li Z et al (2014) Evaluation of conventional, dynamic contrast enhanced and diffusion weighted MRI for quantitative Crohn's disease assessment with histopathology of surgical specimens. Eur Radiol 24:619–629
10. Zhu J, Zhang F, Luan Y et al (2016) Can Dynamic Contrast-Enhanced MRI (DCE-MRI) and Diffusion-Weighted MRI (DW-MRI) Evaluate Inflammation Disease: A Preliminary Study of Crohn's Disease. Medicine (Baltimore) 95:e3239
11. Ziech ML, Lavini C, Bipat S et al (2013) Dynamic contrast-enhanced MRI in determining disease activity in perianal fistulizing Crohn disease: a pilot study. AJR Am J Roentgenol 200:W170–W177
12. Bhatnagar G, Dikaios N, Prezzi D, Vega R, Halligan S, Taylor SA (2015) Changes in dynamic contrast-enhanced pharmacokinetic and diffusion-weighted imaging parameters reflect response to anti-TNF therapy in Crohn's disease. Br J Radiol 88:20150547
13. Zhu J, Zhang F, Zhou J, Li H (2017) Assessment of therapeutic response in Crohn's disease using quantitative dynamic contrast enhanced MRI (DCE-MRI) parameters: A preliminary study. Medicine (Baltimore) 96:e7759
14. Le Bihan D, Breton E, Lallemand D, Aubin ML, Vignaud J, Laval-Jeantet M (1988) Separation of diffusion and perfusion in intravoxel incoherent motion MR imaging. Radiology 168:497–505
15. Koh DM, Collins DJ, Orton MR (2011) Intravoxel incoherent motion in body diffusion-weighted MRI: reality and challenges. AJR Am J Roentgenol 196:1351–1361
16. Freiman M, Perez-Rossello JM, Callahan MJ et al (2013) Characterization of fast and slow diffusion from diffusion-weighted MRI of pediatric Crohn's disease. J Magn Reson Imaging 37:156–163
17. Harvey RF, Bradshaw JM (1980) A simple index of Crohn's-disease activity. Lancet 1:514
18. Yoon K, Chang KT, Lee HJ (2015) MRI for Crohn's Disease: Present and Future. Biomed Res Int 2015:786802
19. Rimola J, Alvarez-Cofino A, Perez-Jeldres T et al (2017) Comparison of three magnetic resonance enterography indices for grading activity in Crohn's disease. J Gastroenterol 52:585–593
20. Hectors SJ, Besa C, Wagner M et al (2017) DCE-MRI of the prostate using shutter-speed vs. Tofts model for tumor characterization and assessment of aggressiveness. J Magn Reson Imaging 46:837–849
21. Li X, Priest RA, Woodward WJ et al (2013) Feasibility of shutter-speed DCE-MRI for improved prostate cancer detection. Magn Reson Med 69:171–178
22. Rohrer M, Bauer H, Mintorovitch J, Requardt M, Weinmann HJ (2005) Comparison of magnetic properties of MRI contrast media solutions at different magnetic field strengths. Investig Radiol 40:715–724
23. Zhang X, Petersen ET, Ghariq E et al (2013) In vivo blood T(1) measurements at 1.5 T, 3 T, and 7 T. Magn Reson Med 70:1082–1086
24. Sourbron SP, Buckley DL (2011) On the scope and interpretation of the Tofts models for DCE-MRI. Magn Reson Med 66:735–745
25. Dyvorne HA, Galea N, Nevers T et al (2013) Diffusion-weighted imaging of the liver with multiple b values: effect of diffusion gradient polarity and breathing acquisition on image quality and intravoxel incoherent motion parameters–a pilot study. Radiology 266:920–929
26. Orton MR, Collins DJ, Koh DM, Leach MO (2014) Improved intravoxel incoherent motion analysis of diffusion weighted imaging by data driven Bayesian modeling. Magn Reson Med 71:411–420
27. Danese S, Sans M, de la Motte C et al (2006) Angiogenesis as a novel component of inflammatory bowel disease pathogenesis. Gastroenterology 130:2060–2073
28. Carr ND, Pullan BR, Schofield PF (1986) Microvascular studies in non-specific inflammatory bowel disease. Gut 27:542–549
29. Oto A, Zhu F, Kulkarni K, Karczmar GS, Turner JR, Rubin D (2009) Evaluation of diffusion-weighted MR imaging for detection of bowel inflammation in patients with Crohn's disease. Acad Radiol 16:597–603
30. Dohan A, Taylor S, Hoeffel C et al (2016) Diffusion-weighted MRI in Crohn's disease: Current status and recommendations. J Magn Reson Imaging 44:1381–1396
31. Wagner M, Ko HM, Chatterji M et al (2018) Magnetic resonance imaging predicts histopathologic composition of ileal Crohn's disease. J Crohns Colitis. https://doi.org/10.1093/ecco-jcc/jjx186
32. Li XH, Mao R, Huang SY et al (2018) Characterization of Degree of Intestinal Fibrosis in Patients with Crohn Disease by Using Magnetization Transfer MR Imaging. Radiology 287:494–503